Supercell tornadoes are much stronger and wider than damage-based ratings indicate

Joshua Wurman[a,1,2], Karen Kosiba[a,1], Trevor White[a,1], and Paul Robinson[a,1]

[a]Center for Severe Weather Research, Boulder, CO 80305

Edited by Kerry A. Emanuel, Massachusetts Institute of Technology, Cambridge, MA, and approved January 25, 2021 (received for review October 15, 2020)

Tornadoes cause damage, injury, and death when intense winds impact structures. Quantifying the strength and extent of such winds is critical to characterizing tornado hazards. Ratings of intensity and size are based nearly entirely on postevent damage surveys [R. Edwards et al., *Bull. Am. Meteorol. Soc.* 94, 641–653 (2013)]. It has long been suspected that these suffer low bias [C. A. Doswell, D. W. Burgess, *Mon. Weather Rev.* 116, 495–501 (1988)]. Here, using mapping of low-level tornado winds in 120 tornadoes, we prove that supercell tornadoes are typically much stronger and wider than damage surveys indicate. Our results permit an accurate assessment of the distribution of tornado intensities and sizes and tornado wind hazards, based on actual wind-speed observations, and meaningful comparisons of the distribution of tornado intensities and sizes with theoretical predictions. We analyze data from Doppler On Wheels (DOW) radar measurements of 120 tornadoes at the time of peak measured intensity. In striking contrast to conventional damage-based climatologies, median tornado peak wind speeds are ~60 m·s^{-1}, capable of causing significant, Enhanced Fujita Scale (EF)-2 to -3, damage, and 20% are capable of the most intense EF-4/EF-5 damage. National Weather Service (NWS) EF/wind speed ratings are 1.2 to 1.5 categories (~20 m·s^{-1}) lower than DOW observations for tornadoes documented by both the NWS and DOWs. Median tornado diameter is 250 to 500 m, with 10 to 15% >1 km. Wind engineering tornado-hazard-model predictions and building wind resistance standards may require upward adjustment due to the increased wind-damage risk documented here.

tornado | natural hazards | climatology | wind damage

Tornadoes cause direct harm to people, infrastructure, and communities (1). Quantifying tornado risk requires accurate knowledge of their wind speeds and the size of the areas at risk from these intense winds. However, since direct measurements of tornado winds are rare, tornado intensity and size are nearly always inferred indirectly from postevent damage surveys applying the Fujita (F) or Enhanced Fujita (EF) scales (2–5) to infer maximum wind speeds. Statistics concerning tornado frequency, intensity, and size are derived from these surveys. However, because most tornadoes do not damage well-engineered structures, from which the most intense wind speeds can be inferred, and many occur in primarily rural areas, damage-based tornado wind speed and size estimations are likely severely low biased (6–11). A limited climatology (12), using Doppler On Wheels (DOW) radar data (13–15), suggested that tornadoes may be larger and more intense than indicated by these surveys. In-situ observations of wind speeds reliably demonstrable to be inside the radius of maximum winds of tornadoes are very rare (16, 17) and inadequate for deriving a statistically meaningful climatology. It is no exaggeration to state that, until now, statistics concerning even the most basic characteristics of tornadoes, including intensity and size, could not be quantified with confidence.

DOW Tornado Data in 120 Tornadoes

DOWs conducted thousands of wind mapping cross-sections through 140 supercell* tornadoes over the Plains of the United States from 1995 to 2006 (18, 19), occasionally permitting comparisons of wind measurements to observed damage (16–18, 20, 21) (Fig. 1), enabling us to create a mobile radar-based climatology of tornado characteristics immune to the biases associated with damage-based studies.

Maps of DOW-measured Doppler wind velocities (V_d) are used to identify tornado center locations and diameters (X_d), determine propagation velocity (V_p), and calculate peak ground-relative wind speeds (V_{gmax}) (see *Materials and Methods*). Results are filtered by altitude above radar level (ARL) with thresholds at 500 m (120 cases), 60 m (28 cases), and using a combined observation resolution/height filter, 200 m and $X_d/B \geq 4$ ("Tier 1," 40 cases), where B is half-power (3 dB) radar beamwidth. Filtering by altitude improves representativeness compared to near-surface winds impacting structures. Filtering by resolution retains only cases where small-scale variability and strong gradients in tornado wind fields are well resolved. We report tornado metrics for these filtering criteria using triplet notation (500 m ARL, Tier 1, <60 m ARL).

Results and Discussion

DOW-Measured Tornado Intensity. Median V_{gmax} of the DOW-observed tornadoes are 57, 59, and 64 m·s^{-1}, with a maximum of 144 m·s^{-1} observed at 37 m ARL. The National Weather Service (NWS) assigns an EF (F before January 2007) intensity and path-width ratings based on observed damage, aggregated and archived by the NWS Storm Prediction Center (SPC) in the "OneTor" database (22). Histograms of DOW V_{gmax}, binned by NWS EF wind-speed ranges, to facilitate comparisons, show relatively broad peaks at wind speeds corresponding to EF-2/EF-3 intensity, for all filtering criteria (Fig. 2). Cases filtered to include only tornadoes observed below 60 m ARL exhibit median V_{gmax} = 64 m·s^{-1}, slightly stronger than the 57 m·s^{-1} observed for all tornadoes observed below 500 m

Significance

This study documents the actual distribution of supercell-tornado wind intensities and sizes, revealing that most are much stronger than damage surveys indicate, with >20% of tornadoes potentially capable of causing catastrophic EF-4/EF-5 damage. Additionally, supercell tornadoes are shown to be much wider than damage surveys indicate. These results are significant for tornado science, tornado risk quantification and mitigation, and design for more resilient communities. We also present meaningful comparisons of the distribution of actually observed tornado intensities and sizes with theoretical predictions, which is significant for basic tornado science.

Author contributions: J.W. designed research; J.W. and K.K. performed research; J.W., K.K., T.W., and P.R. analyzed data; and J.W. and K.K. wrote the paper.

The authors declare no competing interest.

This article is a PNAS Direct Submission.

[1]Present address: Department of Atmospheric Sciences, University of Illinois, Urbana, IL 61801.

[2]To whom correspondence may be addressed. Email: jwurman@illinois.edu.

Published March 22, 2021.

*This study analyzes data from supercell-spawned mesocyclonic tornadoes. Landspout and gustnado-type vortices were excluded.

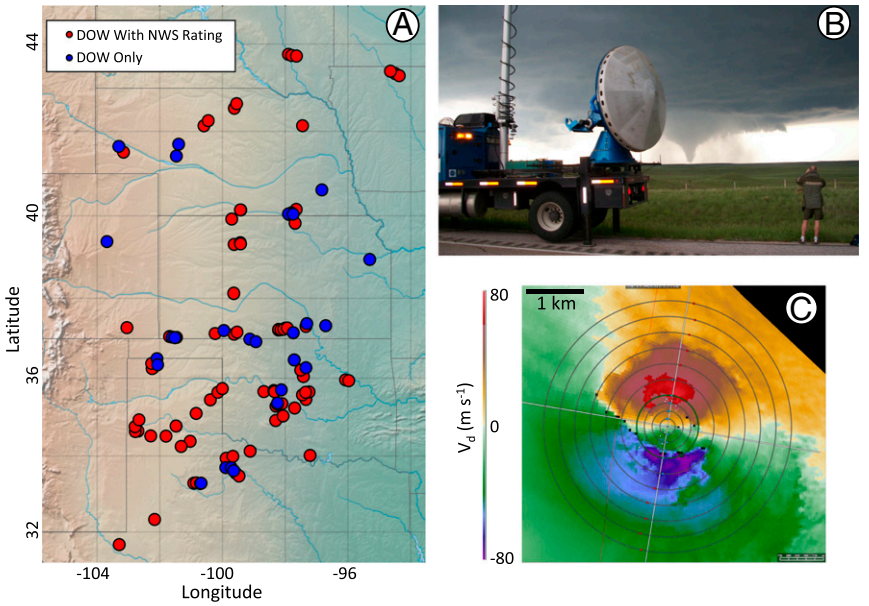

Fig. 1. DOW mapping of tornado winds. (*A*) Location of 120 tornadoes observed by DOW from 1995 to 2006, showing 82 cases for which NWS ratings are identified (red). (*B*) DOW scanning a tornado. (*C*) Example of DOW V_d map of a tornado. Blue/red shading is V_d toward/away from radar. The thickest ring encloses region defined by X_d.

ARL, consistent with case-study results suggesting tornado winds are strongest near the ground (16–18, 23). Strikingly, DOW observations indicate that 21, 20, and 25% of supercell tornadoes are potentially "violent" and capable of causing EF-4/EF-5 damage. This is in stark contrast to NWS tornado intensity statistics, which indicate roughly exponential decline in frequency from EF-0 to EF-5, for tornadoes occurring in the DOW core study period (months of May and June in 1995 to 2001 and 2003 to 2005) and area (Texas, Oklahoma, Kansas, and Nebraska), with only 1% rated by NWS as EF-4/EF-5. In order to mitigate the effects of potential DOW sampling bias (discussed below), NWS ratings are identified for 82 of the DOW-observed tornadoes (see *Materials and Methods*), revealing an exponential but shallower decline in frequency from EF-0 to EF-5, with 7% rated EF-4/EF-5. The median V_{gmax} of the 82 DOW-observed tornadoes matched with corresponding damage ratings are stronger, 61, 68, and 71 m·s^{-1},

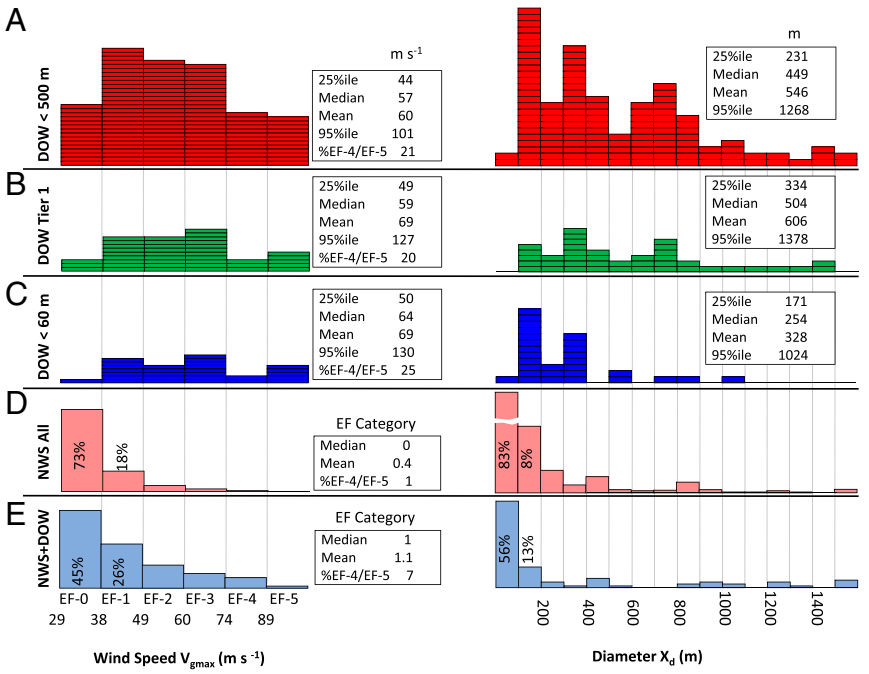

Fig. 2. Histograms of DOW and NWS tornado intensity and width ratings reveal that supercell tornadoes are much stronger and larger than indicated by NWS statistics. (*A*) All DOW cases <500 m ARL, (*B*) DOW Tier 1, and (*C*) DOW <60 m ARL. (*D*) All NWS ratings in study area/period. (*E*) NWS cases (82) observed by DOW.

compared to 57, 59, and 64 m·s^{-1} for all DOW-observed tornadoes.

The differences between the intensity distributions based on DOW versus NWS ratings are visually clearly evident and are rigorously confirmed with a Mann–Whitney *U* test and the two-sample Kolmorogov–Smirnov test of the 82 sample distributions. A Mann–Whitney *U* test reveals a *U* value of 1,598, z of −5.9, and p of 1.5×10^{-9}, which leads to rejecting the null hypothesis that the NWS and DOW intensity distributions are the same. The two-sample Kolmogorov–Smirnov test yields a D value of 4, which also leads to rejecting the null hypothesis that the NWS and DOW intensity distributions are the same.

Comparison of individual NWS and DOW EF ratings reveals mean NWS underestimates of 1.5, 1.5, and 1.6 categories, with 77, 86, and 80% underestimated by one or more EF category, and 23, 18, and 25% underestimated by three or more EF categories (Fig. 3). NWS EF ratings are integral, with coarse and variable spacing between category thresholds and no upper bound for EF-5, but approximate wind speed values can be reasonably assigned to NWS EF ratings (see *Materials and Methods*). Using this method, the mean difference between DOW-observed and NWS-rated wind speeds for the 82 tornadoes is 20 m·s^{-1}, and for a subset of 45 tornadoes rated EF-1 or higher by NWS, the difference is 19 m·s^{-1}. (Note that this 19 m·s^{-1} difference corresponds to 1.2 EF categories due to wider EF binning for higher EF categories.) One example of a significant difference between DOW and NWS ratings is a small, but intense, tornado observed by DOW in rural Nebraska on 22 May 2004. Peak DOW-measured V_d = 72 m·s^{-1} at 40 m ARL, with V_{gmax} = 82 m·s^{-1}, corresponds to EF-4 intensity, whereas the NWS rating was EF-0. While this discrepancy may have been due to a lack of a detailed damage survey, resulting in a default EF-0 NWS rating, we found many examples, with NWS EF ratings of ≥EF-1 (Fig. 3), with 2 to 3 category and/or >40 m·s^{-1} under ratings by NWS compared to DOW observations. Very few tornadoes, 6, 4, and 0%, are rated lower from DOW observations compared to NWS.

Potential Biases in Damage-Based and DOW Sampling of Tornado Intensity. Both damage and DOW-based statistics suffer from potential observational and selection biases.

During the study period, DOWs sampled supercell tornadoes occurring exclusively in the Plains of the United States and adjacent regions, excluding those occurring in other regions, notably the Southeastern region of the United States (Fig. 1). The Plains provide a comparatively easy logistical environment in which to obtain low-level tornado observations because of several factors. Flatter terrain, fewer trees, and fewer buildings combine to facilitate near-horizon scanning by truck-borne radars such as DOWs. The much lower population density in the Plains results in faster average safe driving speeds, facilitating the "chasing" of potentially tornadic storms. There is no evidence that the intensity distributions of tornadoes spawned by warm season supercells in the Plains are significantly different from those occurring elsewhere, so it is believed that the results presented here are generally representative. While Plains-only sampling could, potentially, introduce bias, it is currently unavoidable since no comparable dataset of direct observations of wind speeds in the very lowest levels of tornadoes exists.

This study focuses on the observed properties of warm season supercell-spawned tornadoes, excluding other types. Tornadoes spawned from quasi-linear convective systems (QLCS) (24–27), nonsupercell thunderstorms (28), and tropical cyclones (29, 30) generally have shorter forecast lead times and lifespans, making mapping of low-level wind speeds much more difficult and infrequent. While the impacts of nonsupercell tornadoes can be significant, supercell-spawned tornadoes are overwhelmingly the type responsible for damage and death, in both the Plains and Southeast (31, 32), and are the most intense (33, 34).

Intense tornadoes crossing rural areas often do not cause significant damage, or only damage weaker structures, and are not rated as intense by NWS. The strong tornado illustrated in Fig. 3 was small and crossed over very open terrain, nearly devoid of structures. Some, particularly weaker or short-lived, rural tornadoes may never be noticed or logged by NWS. Damage caused by some rural tornadoes occurring during the study period was not formally surveyed, and these tornadoes were given default EF-0 ratings by NWS. Population density in the study area, and the

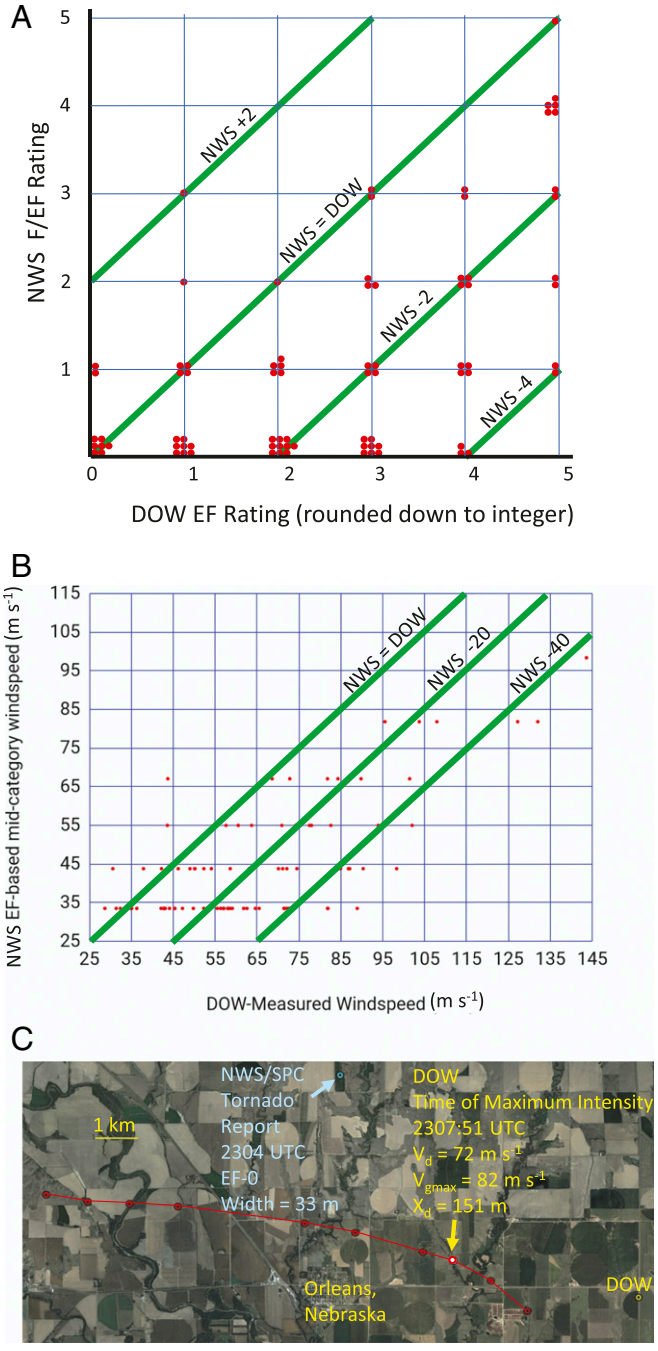

Fig. 3. Comparison of individual DOW and NWS intensity ratings. (*A*) Scattergram comparing DOW versus integral NWS ratings. (*B*) Comparison of DOW versus NWS speeds. NWS ratings average 1.2 to 1.5 categories, about 20 m·s^{-1} lower than DOW observations, with extreme differences up to 4 categories and 50 m·s^{-1}. (*C*) Example of an intense DOW-measured 72 m·s^{-1} tornado, crossing rural terrain on 22 May 2004, rated EF-0 by NWS.

resulting fractional area covered with structures capable of sustaining damage capable of being rated by NWS, is low compared to other tornado-prone regions of the United States, particularly the Southeast. Therefore, it is likely that the underrating of tornado intensity in the Southeast or other densely populated regions is less than reported here.

The higher frequency of "violent" NWS ratings of tornadoes also observed by DOW (7% EF-4/EF-5) compared to NWS ratings of all tornadoes in the study area/period (1% EF-4/EF-5) is evidence of some DOW sampling bias. DOW missions specifically target supercell thunderstorms, not nonsupercell and QLCS systems. DOW missions attempt to target "better" storms and operate when and where the forecast is indicative of more intense tornadoes. These combine to cause the difference in the distribution of NWS ratings of all tornadoes in the study area compared to the NWS ratings of just DOW-sampled cases. By comparing the intensity distribution of only the 82 tornadoes documented by both DOW and NWS, all supercell spawned, the potential effects of DOW sampling biases are eliminated. [After the study period, beginning about 2009, the NWS began testing an experimental Damage Assessment Toolkit that maps damage within a tornado, potentially facilitating more detailed point-by-point comparisons of DOW and NWS observations in rare cases with extremely granular damage surveys. This level of damage survey detail was not available for this study except in isolated cases (20, 35).]

The finest-scale radar observations of the most intense tornadoes represent very short-duration wind gusts, sometimes <1 s (21). But the wind-gust duration required to cause observed structural damage is not well known. These factors could cause intensity overestimation (36). The axisymmetric vortex assumption used here while calculating V_{gmax} from V_d and V_p, adjusting for the unobserved component of the full vector wind field, can introduce error, as can corrections for observational resolution assuming sharply peaked undersampled wind-speed maxima (see *Materials and Methods*). However, without any adjustments for undersampling or unobserved components, median raw observed peak V_d, almost certainly underestimates of true tornado intensity, are 46, 48, and 51 $m{\cdot}s^{-1}$ with EF-4/EF-5 indicated for 13, 18, and 21% of tornadoes, still strikingly stronger than indicated by NWS damage-based ratings.

Conversely, most aspects of DOW sampling lead to underestimation of intensity. These include contamination of measurements by ground clutter, weighting of V_d toward centrifuged scatters such as rain, hail, and debris (37), coarse temporal sampling leading to substantial chances of V_{gmax} occurring between observation times and, in some cases, no DOW observations during peak tornado intensity. While the dependence of V_{gmax} on height is not well known, there is evidence suggesting that wind speeds are nearly constant or slightly decrease with increasing height above 5 to 10 m ARL (16, 17, 23, 38, 39). Therefore, the DOW measurements used here, obtained >10 m in all but two cases, and mostly from >60 m, are likely representative, or underestimates, of V_{gmax} at 5 to 10 m ARL. Some very weak, invisible, marginal, or not formally reported by NWS, DOW-observed tornadoes (17) are included in this study, reducing median V_{gmax} by a few $m{\cdot}s^{-1}$. Finally, for some DOW-observed tornadoes, where V_p or its relationship to observational geometry could not be confidently determined, V_p was cautiously set to 0.0 $m{\cdot}s^{-1}$, resulting in underestimations of V_{gmax}.

DOW-Measured Tornado Size. Median X_d for DOW-observed tornadoes are 449, 504, and 254 m. Lower X_d for tornadoes observed <60 m ARL, necessarily at close range, are likely due to DOW crews avoiding deployments very near to very wide tornadoes. Histograms (Fig. 2) reveal frequency peaks of X_d at about 150, 350, and 750 m. In striking contrast, NWS reports median $X_d < 100$ m.

The complex structure of tornado wind fields, resulting damage, and differing definitions of X_d complicate comparison of DOW and NWS X_d. NWS X_d are maximum widths of damage swaths, while DOW X_d are distances across regions containing maximum observed winds, at the time of maximum observed wind speeds. During intense tornadoes, damage potential exists well outside the region defined by DOW X_d (20, 21). In weak/marginal tornadoes, damage potential exists only in narrow strips, with widths $<<X_d$, on the strong (right side relative to V_p) sides, where V_p adds constructively to the tangential winds, V_t, of tornado vortices, resulting in the strongest V_{gmax}. After these weaker tornadoes, and for tornadoes occurring over rural areas, damage-based X_d may not be well documented, and NWS may assign minimum nominal values for X_d. In addition, some tornadoes exhibit multiple scales of motion, with multiple wind-speed maxima rings or regions, the intensity of which, and even existence, is sometimes transient (19). The DOW-documented multimodal distribution of X_d suggests that there are preferred spatial scales for these rings. Outer rings can exhibit stronger, potentially more damaging wind speeds, compared to inner rings. The visual scale of tornadoes (typically condensation funnels) can differ significantly from damage-determined or radar-determined X_d (19). Additionally, the maximum X_d reported by NWS may not occur at the time of maximum intensity.

DOW measures X_d well above the typical height of damaged structures, and tornadoes appear visually to increase in size with height. However, this is likely at least partially a visual illusion based on increased condensation funnel diameter and/or centrifuging debris spiraling away from the center of the tornado as it rises. Case-study results (40–44) suggest that X_d may not systematically increase from 50 to 500 m above ground level (AGL). Some suggest that tornadoes may narrow a few tens of meters in the few tens of meters closest to the ground, and/or that radar measurements may slightly overestimate X_d when significant debris is lofted (37, 41). In one case study which analyzed near-ground DOW observations over a dense array of damaged structures, DOW and damage-indicated X_d only differed by a few tens of meters (20). Therefore, DOW measurements of X_d are likely closely representative, or only slightly wider than, the near-ground X_d. Even if plausible tapering corrections are made to DOW-measured X_d, median DOW-measured X_d >> damage-indicated X_d.

There is only a very weak negative correlation between tornado size and intensity at the time of peak intensity (Fig. 4), in contrast to the positive correlations found using damage-survey statistics (45). On average, wider tornadoes are not stronger than narrower tornadoes. Nevertheless, 3, 5, and 4% of tornadoes are both very wide and very intense, exhibiting $X_d > 1$ km at the time that $V_{gmax} > 74$ $m{\cdot}s^{-1}$ (EF-4/EF-5 equivalent), likely dozens of tornadoes annually. While there is no established relationship between tornado-wind duration and resulting damage, larger tornadoes are likely to result in longer durations of intense winds and airborne debris effects. As urban/suburban areas spread, there is an increasing likelihood of such extremely wide and intense tornadoes impacting broad swaths of densely populated areas, risking widespread catastrophic damage over many square kilometers (1, 23). Wind engineering tornado-hazard-model predictions and building wind-resistance standards may require upward adjustment due to the increased wind-damage risk documented here.

Observed versus Predicted Tornado Intensity and Size. Properties endemic to storms and storm environments such as storm geometry and/or available energy can be used to predict expected values of tornadic intensity and size (46–50). Assuming commonly cited parameters (e.g., convective available potential energy [CAPE] = 2,700 $J{\cdot}kg^{-1}$, mesocyclone radius [R] = 2 km, and mesocyclone vertical vorticity [ξ] = 0.01 s^{-1}), theoretical and modeling considerations suggest characteristic $V_t = 52$ $m{\cdot}s^{-1}$ and $X_d = 550$ m. Since V_t and V_p add constructively on the strong side of tornadoes, and V_p averages 10 $m{\cdot}s^{-1}$, the prediction of typical $V_t = 52$ $m{\cdot}s^{-1}$

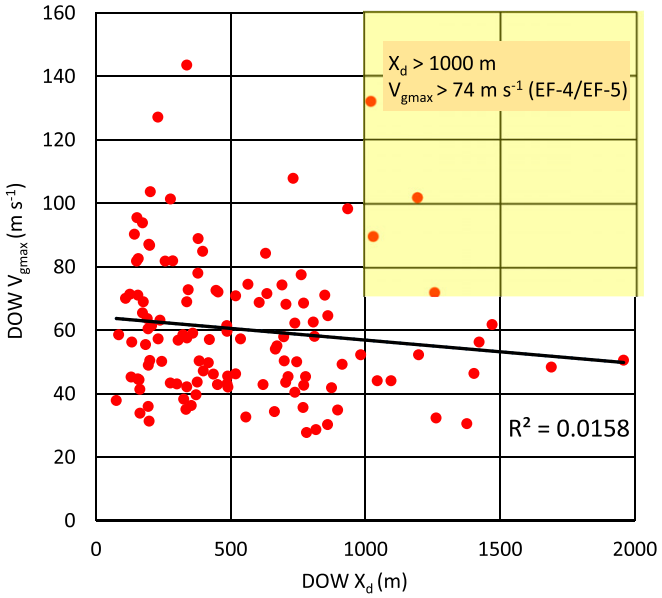

Fig. 4. DOW-measured tornado peak intensity (V_{gmax}) versus size (X_d) at the time of V_{gmax}. There is only a very weak and negative correlation between tornado intensity and size. A small but important fraction of tornadoes, about 4%, are simultaneously X_d > 1 km and V_{gmax} > 74 m·s^{-1} (yellow shaded region).

is consistent with the DOW-observed median V_{gmax} = 57, 59, and 64 m·s^{-1}. Similarly, predicted X_d = 550 m, is consistent with median DOW X_d = 449, 504, and 254 m, except for cases filtered for observations <60 m ARL, where safety concerns likely resulted in a DOW selection bias favoring small tornadoes. Various assumptions and unknowns about wind profiles, vortex structure, and storm environment cause predicted intensity and size to vary substantially, and some predictions may not include near-surface tapering effects. DOW and other observations suggest substantial variability with V_{gmax} ranging from 27 to 144 m·s^{-1} and X_d varying from 76 to 1,958 m in this climatology and in case studies (19, 21, 23, 51–57). Higher CAPE results in substantially higher predictions for V_t but not nearly as high as those observed by DOWs in the most intense tornadoes. However, these maximum predicted V_t have been demonstrated to be exceedable, possibly by substantial amounts (48). However, only unusually extreme values of CAPE, R, and ξ combine to result in predictions for X_d as low as the 25th percentile of DOW observed X_d = 231, 334, and 171 m (Fig. 2) or the tornado with X_d = 151 m (Fig. 3*C*). For example, even CAPE = 5,000 J·kg^{-1}, R = 2 km, and ξ = 0.005 s^{-1} results in predicted X_d = 200 m.

While general consistency between predictions of intensity and, to some extent, size, with the median of DOW observations are shown, there is little predictive value for individual tornadoes. DOW measured X_d and V_{gmax} of different tornadoes, on the same day, sometimes simultaneously spawned from the same thunderstorm in seemingly similar atmospheric environments, can vary considerably. Other factors, for example storm updraft diameters (58), may influence individual tornado intensities. Nevertheless, this current analysis presents meaningful comparisons between predictions and the actual distribution of tornado intensities and sizes.

DOW-Calculated Tornado Central Pressure Deficit and Divergence. DOW observations permit quantification of many tornado properties. Rapid drops in pressure during tornadoes may result in stress on sealed buildings. Rare pressure measurements have revealed pressure drops ranging from 2,000 to 10,000 Pa (59–61), while theoretical predictions predict cyclostrophic pressure deficits, Δ-P_c ~1,000 to 14,000 Pa (40). DOW-derived median and mean Δ-P_c at the time of maximum intensity, at the altitude of V_{gmax}, are 1,620, 1,890, and 2,483 Pa and 2,837, 3,704, and 4,283 Pa, respectively, with an extreme of 19,360 Pa. Ten percent exceed Δ-P_c of 5,669, 7,681, and 10,534 Pa. [A pressure deficit report (62) of 19,400 Pa in a moderate-intensity tornado, with a measured V_g = 50.4 m·s^{-1}, is inconsistent with our measurements, theoretical predictions (41), and other in-situ observations, some in intense tornadoes (59–61).]

In well-resolved (Tier 1) tornado cases, median divergence of V_d calculated within the region defined by X_d, and in a narrower region within X_d/2, is +0.01 s^{-1}. Adjusted for particle centrifuging at 5 m·s^{-1} (37), median air-parcel divergence is −0.02 s^{-1} (within X_d) and −0.04 s^{-1} (within X_d/2), with <0.0 s^{-1} observed in more than 60% of cases (see *Materials and Methods*), suggesting that, at least at the time of maximum intensity, most tornadoes contain central updrafts near the surface. Direct comparison with updrafts/downdrafts inferred in individual case studies is challenging due to varying analysis assumptions, altitude and duration of observations, and possible case study selection bias. Case studies that consider centrifuging suggest central updrafts exist during some portions of tornado life cycles (17, 18), and that substantial convergence or divergence may exist below typical DOW-observation levels, affecting inferred vertical wind speeds.

Discussion Summary

Supercell tornadoes are, in general, much more intense and wider than damage surveys indicate. Direct comparison among 82 supercell tornadoes both observed by DOW and rated by NWS reveals a significant, 20 m·s^{-1} 1.5 EF category, discrepancy between DOW and NWS reported intensities. For the 45 DOW-observed tornadoes rated EF-1 or higher by NWS, the difference is 19 m·s^{-1} and 1.2 EF categories. While there may be biases due to sampling in both DOW and NWS data, this one-to-one comparison of 82 and 45 tornadoes demonstrates that NWS ratings are systematically and significantly too low. This has implications for risk assessment and mitigation. Hazard maps should be updated to include this reality. Building codes should be informed by these higher risks. From a forecasting and operational perspective, these results show that weak and actually narrow wind field supercell-spawned tornadoes are uncommon; most tornadoes are capable of producing very severe damage, with >20% capable of causing catastrophic EF-4/EF-5 damage. We show that, at the time of maximum measured intensity, narrow wind field tornadoes are as likely to be as intense as wide tornadoes. While current tornado warnings advise strong precautions against all tornadoes, communication of these results to the public may encourage more attentive responses.

Materials and Methods

Navigation of DOW Data. DOW radars have collected data in tornadoes since 1995. V_d data from several individual DOW case studies, typically of intense, high-impact, or otherwise unusual tornadoes, have been navigated, processed, and analyzed in detail prior to this study (18, 20, 41, 63–70). Other groups have reported case-study observations of tornadoes, resolving tornado metrics in some instances (52–55). Some analyses have included comparisons with damage (16, 17, 20, 35, 56, 57). These reported analyses are case studies purposely selected based on tornado intensity or impact and represent a sampling of exceptional tornadoes. For this climatological study, quality-controlled data from previous DOW studies, as well as from all additional tornadoes observed by DOWs during 1995 to 1999 and 2001 to 2006, are included.

Navigation of DOW data were achieved through a combination of Global Positioning System (GPS) locations and mapping of ground-clutter targets. In most cases, data are from stationary leveled deployments when antenna pitch and roll were less than 0.2° as measured by precision bubble levels inside and near the antenna pedestals. During 1995 to 1999, and for a few cases during 2001 to 2005, data collected while DOWs were mobile are included. Mobile data are level within about 1° at nearly all times, apart from short-duration potholes, railroad crossings, turns, etc., which were excluded from the analysis. V_d were filtered using signal quality, de-aliasing, removal of nonmeteorological targets, and when necessary, corrected for vehicle motion. When radar beam

elevations are <B, a Gaussian-weighted correction raises the effective elevation angle such that they asymptote at 0.3° to account for terrain, tree, and structural blockage of the bottom portion of beams, resulting in the effective elevation angle of a beam nominally pointing at 0.0° elevation being adjusted to 0.34°.

In this analysis, data are characterized by altitude ARL. When the ground altitude under a tornado is different from that under a DOW, ARL and AGL values will be different. This is rarely significant in the relatively flat terrain of the Plains, and at the close ranges, over which most DOW tornado data are collected. Also, given the typically short ranges, nonlinear propagation of radar beams is neglected, except for the adjustment for blockage of the lower portion of ground-skimming beams discussed above.

The GURU software suite, developed by the Center for Severe Weather Research, was used to analyze 5,614 cross-sections through candidate tornado vortices. For each cross-section containing data in a candidate tornado vortex, in GURU, the authors enter a first-guess center location and outline an ∼2 km region enclosing the vortex. These are then used by GURU to calculate refined center locations, X_d and V_p. Automatically determined center positions and X_d are reviewed by the authors and refined as necessary. Sometimes this was required for complex vortices, containing subvortices or multiple wind-speed maxima. In some cases, the determination of whether vortices were independent tornadoes or subvortices within multiple-vortex mesocyclones (19, 21, 41) was subjective. Centers, V_d fields, and V_p were used to automatically identify cross-sections containing V_{gmax}, which are used in this study.

Vortices are characterized as tornadoes when the maximum velocity difference across them is >40 m/s within a <2 km region (19, 39), are associated with a mesocyclone and/or hook echo of a supercell thunderstorm (71), and are not close to and/or associated with other tornadoes, thus excluding vortices along proximate gust fronts ["gustnadoes" (28)] and nearby anti-cyclonic vortices (19). Vortices not observed below 500 m ARL are also rejected. From 140 candidate tornadoes, 120 are selected for analysis in this study.

Calculation of Tornado Metrics. The time of maximum observed intensity (defined as the time of peak V_{gmax}) and various metrics of the wind field, including V_p, V_{gmax}, Δ-P_c, and divergence, are calculated for each tornado. Some DOW-observed tornadoes may not be observed at the time of maximum actual intensity. In some cases, V_p cannot be determined from DOW measurements. This can occur because of irregular cross-section scheduling or the existence of only a single cross-section through the tornado. In such cases, when possible, V_p are estimated from mesocyclone motion as measured by operational NWS WSR-88D radars. Otherwise, V_p is set to zero. V_p is set to zero for data collected while DOWs are mobile, except in a few cases where precise navigation is possible.

Divergence within the region defined by X_d is calculated by $2 \times (\Delta\text{-}V/\Delta\text{-}X) \sin(\gamma)$, where Δ-V is the difference between the maximum aspect ratio adjusted extrema (inbound and outbound) of V_d observed on either side of the tornado in a circle defined by X_d, Δ-X is the distance between these extrema, and γ is the phase offset angle (zero pointing from the center of the tornado back to the DOW) of a least-squares sine wave fit to the V_d values along the ring.

Cyclostrophic pressure deficits (Δ-P_c) at the center of every tornado are calculated using an analytic formula (40):

$$\frac{1}{\rho}\Delta P_c = -\frac{1}{2}V_{gmax}^2 + \frac{V_{gmax}^2}{2b}\left[\left(\frac{X_d}{2r}\right)^{2b} - 1\right],$$

which assumes a modified Rankine vortex with an exponential decay parameter outside of the radius of maximum winds of b = 0.6, calculated compared to a range of $r = 2 \times X_d$ from the tornado center, and atmospheric density, ρ = 1 kg·m^{-3}. Typical values for this decay parameter from case studies are 0.5 to 0.8 (40, 41, 51, 67, 70). V_t is calculated from the difference between the maximum aspect ratio adjusted extrema (inbound and outbound) of V_d observed on either side of the tornado.

Adjustment for Observation Resolution and Unobserved Components of Wind Velocity. Following standardized procedures, our analysis adjusts V_d for the effects of coarse spatial sampling and inferred unobserved V_{gmax} due to V_p. V_d are corrected for aspect ratio sampling error, (39, 41, 51, 72) by multiplying by $1/(1-0.48(B/X_d))$. This adjustment is capped at 1.086, equivalent to what would be applied for $B/X_d > 6$, to arrive at a temporary product, adjusted velocity, V_{da}. V_d is a measure of only the toward/away component of the full wind-velocity vector since Doppler radars do not sample the component of motion perpendicular to radar beams. For tornadoes propagating at any appreciable angle to the radar beams, the unobserved component of the wind velocity vector, $V_p \sin(\theta)$ where θ is the angle between V_p and the radar-beam pointing angle, is significant. To account for this, $V_{gmax} = V_{da} + V_p \sin(\theta)$. The median V_p is 10 m·s^{-1} at the time of maximum intensity, with an extreme of 25 m·s^{-1} consistent with that found in individual case studies. The corrections applied to V_d through this process are usually substantially less than V_p due to multiplication by $\sin(\theta)$. As stated above, no correction is applied to data collected while the DOWs are mobile unless precise navigation is available, or if V_p or $\sin(\theta)$ are not known with confidence, due to uncertain DOW angular navigation or limited duration of observations.

Matching of NWS-Rated Tornadoes and DOW-Observed Tornadoes. In order to compare NWS and DOW ratings of tornado intensity and width, DOW-observed tornadoes are paired with the same tornadoes as reported and rated in the SPC OneTor (22) archive. However, because of the qualitative differences in the DOW and SPC datasets, pairing is sometimes challenging and sometimes cannot be accomplished with confidence.

NWS reports, particularly early in the study period, often relied on tornado spotter, tornado chaser, law enforcement, and media reports of tornado locations and times. These estimations were often subjective and prone to observational bias and other errors. Observers frequently did not have the benefit of GPS locations and estimated their locations and the directions and ranges to tornadoes subjectively. Some tornadoes observed by the DOWs went otherwise unobserved and were not recorded in the SPC database. Some, usually weaker, DOW-observed tornadoes, with well-defined and moderately intense rotation very near the surface, did not have clear visual manifestations such as condensation funnels or lofted dust and were otherwise unobserved or unreported by spotters, chasers, or law enforcement. Some DOW-observed tornadoes occurred inside regions with opaque precipitation, or at night, or were otherwise not optically visible to nonradar equipped observers. When several tornadoes occurred in close proximity and time, tornado identifications could be conflated or artificially split. When supercell thunderstorms produce more than one tornado (cyclic tornadogenesis), it is difficult, solely from visual observations and/or postevent damage surveys, to determine when one tornado ends and another begins. Thus, there are cases in the SPC database in which individual tornadoes, as characterized using DOW observations, are split into multiple SPC-logged events and, conversely, cases in which separate tornadoes, as characterized by DOW observations, are merged into one SPC report.

Prior to 2013, during the period in which the data used in this study were collected, NWS sometimes considered information additional to damage when developing ratings. In several cases, NWS considered using and/or used DOW wind observations when rating tornado wind speeds and tracks, and for parsing in the case of multiple tornadoes. This likely reduced the differences between DOW and NWS ratings in these cases.

DOW data, while collected by skilled teams, occasionally were incorrectly logged, particularly early in the period. During the early years of this study, computer clocks were manually set to coordinated universal time (UTC) by operators, resulting in occasional typographical and other errors in date or time zone. Also, in the early years, GPS locations of DOW deployments were manually logged by operators, then later integrated into the archived data. Similarly, the rotation (parking) angle of the DOWs was manually logged. In most cases, these locations could be verified using ground clutter, intercomparisons between DOWs, independent logs by other operators, drivers, and navigators, and intercomparisons with operational weather radar data. During mobile data collection, extra effort was required to navigate data fields. Thus, most data collected while mobile after 1999 was excluded from this study.

The center locations of each DOW-observed tornado on each mission day were overlaid against NWS-logged tornado locations for those days. NWS records corresponding closely, within several kilometers and several minutes, to DOW tornadoes resulted in DOW/NWS tornado pairings. These pairings were subjectively evaluated by the authors, and only high confidence pairings were retained. Database differences, navigational and reporting errors, and documentation issues resulted in nonpairings for 38 of the 120 analyzed DOW-mapped tornadoes, with 82 DOW-observed tornadoes being paired. As noted in the main text of this report, the median DOW V_{gmax} of paired tornadoes is higher than the overall median. Some of the nonpaired tornadoes were weaker, marginal tornadoes, likely never observed by the public and not entering the SPC database.

Comparing DOW-Observed Winds with NWS EF-Category Grouped Ratings. NWS did not report subcategory distinctions (e.g., fractional F/EF-scale ratings) during the study period, and the EF-scale is not linear, with variably sized binning. Wind speeds can be inferred from NWS ratings, albeit only approximately. We assigned modified midcategory winds speeds to each NWS-rated

tornado (EF-0 = 34 m·s^{-1}, EF-1 = 44 m·s^{-1}, EF-2 = 55 m·s^{-1}, EF-3 = 67 m·s^{-1}, EF-4 = 82 m·s^{-1}, and EF-5 = 98 m·s^{-1}). Since there is no upper limit to EF-5 inferred wind speeds, we assigned 98 m·s^{-1}, corresponding to 220 mph. Results are very insensitive to this value since there is only a single EF-5 NWS-rated tornado in this study. The gross differences between DOW speeds and inferred NWS speeds closely tracks with the integral-EF-category binned comparison, with mean/median = 20/19 m·s^{-1}, which is ~1.5 to 1.8 EF categories, only slightly more than the 1.5 to 1.6 EF category difference resulting from the integrally-binned method. The comparison between methods is also approximate since the wind-speed ranges in different midrange EF bins varies from about 11 to 16 m·s^{-1}.

Data Availability. Data are available via ftp transfer from the publicly accessible DOW Facility data archive by following instructions at the facility web site http://dowfacility.atmos.illinois.edu and/or emailing the lead author.

ACKNOWLEDGMENTS. We thank the many DOW crew and NSF Awards 1447268 and 1361237.

1. W. S. Ashley, S. M. Strader, Recipe for Disaster: How the dynamic ingredients of risk and exposure are changing the tornado disaster landscape. *Bull. Am. Meteorol. Soc.* **97**, 767–786 (2016).
2. T. T. Fujita, *Proposed Characterization of Tornadoes and Hurricanes by Area and Intensity* (SMRP Research Rep. 91, University of Chicago, 1971).
3. Wind Science and Engineering Center, (WSEC), "A recommendation for an enhanced Fujita scale (EF-scale), revision 2" (WSEC, Texas Tech University, Lubbock, TX, 2006). https://www.depts.ttu.edu/nwi/pubs/fscale/efscale.pdf).
4. C. A. Doswell, H. E. Brooks, N. Dotzek, On the implementation of the enhanced Fujita scale in the USA. *Atmos. Res.* **93**, 554–563 (2009).
5. R. Edwards *et al*., Tornado intensity estimation: Past, present, and future. *Bull. Am. Meteorol. Soc.* **94**, 641–653 (2013).
6. D. L. Kelly, J. T. Schaefer, R. P. McNulty, C. A. Doswell III, R. F. Abbey Jr., An augmented tornado climatology. *Mon. Weather Rev.* **106**, 1172–1183 (1978).
7. C. A. Doswell, D. W. Burgess, On some issues of United States tornado climatology. *Mon. Weather Rev.* **116**, 495–501 (1988).
8. H. E. Brooks, C. A. Doswell, M. P. Kay, Climatological estimates of local daily tornado probability for the United States. *Weather Forecast.* **18**, 626–640 (2003).
9. T. A. Coleman, P. G. Dixon, An objective analysis of tornado risk in the United States. *Weather Forecast.* **29**, 366–376 (2014).
10. H. E. Brooks, G. W. Carbin, P. T. Marsh, Increased variability of tornado occurrence in the United States. *Science* **346**, 349–352 (2014).
11. S. M. Strader, W. Ashley, A. Irizarry, S. Hall, A climatology of tornado intensity assessments. *Met. Apps* **22**, 513–524 (2015).
12. C. R. Alexander, J. M. Wurman, "Updated mobile radar climatology of supercell tornado structures and dynamics" in *Presented at 24th Conference on Severe Local Storms* (American Meteorological Society, Savannah, GA, 2008), https://ams.confex.com/ams/24SLS/techprogram/paper_141821.htm.
13. J. Wurman, M. Randall, A. Zahrai, Design and deployment of a portable, pencil-beam, pulsed, 3-cm Doppler radar. *J. Atmos. Ocean. Technol.* **14**, 1502–1512 (1997).
14. J. Wurman, *"The DOW mobile multiple-Doppler network" 30th Conf. on Radar Meteorology* (Amer. Meteor. Soc., Munich, Germany, 2001), pp. 95–97, https://ams.confex.com/ams/30radar/webprogram/Paper21572.html.
15. J. Wurman, M. Randall, "An Inexpensive, Mobile, Rapid-Scan Radar" in *30th International Conference on Radar Meteorology* (Amer. Meteor. Soc., Munich, Germany, 2001), https://ams.confex.com/ams/30radar/techprogram/paper_21577.htm.
16. J. Wurman, K. Kosiba, P. Robinson, In situ, Doppler radar, and video observations of the interior structure of a tornado and the wind–damage relationship. *Bull. Am. Meteorol. Soc.* **94**, 835–846 (2013).
17. K. A. Kosiba, J. Wurman, The three-dimensional structure and evolution of a tornado boundary layer. *Weather Forecast.* **28**, 1552–1561 (2013).
18. J. Wurman, J. M. Straka, E. N. Rasmussen, Fine-scale Doppler radar observations of tornadoes. *Science* **272**, 1774–1777 (1996).
19. J. Wurman, K. Kosiba, Finescale radar observations of tornado and mesocyclone structures. *Weather Forecast.* **28**, 1157–1174 (2013).
20. J. Wurman, C. R. Alexander, The 30 May, 1998 Spencer, South Dakota, storm. Part II: Comparison of observed damage and radar-derived winds in the tornadoes. *Mon. Weather Rev.* **133**, 97–119 (2005).
21. J. Wurman, K. A. Kosiba, P. Robinson, T. Marshall, The role of multiple vortex tornado structure in causing storm researcher fatalities. *Bull. Am. Meteorol. Soc.* **95**, 31–45 (2014).
22. J. T. Schaefer, R. Edwards, "The SPC tornado/severe thunderstorm database" in *Paper presented at the AMS 11th Conf. on Applied Climatology*, (Dallas, TX, 1999).
23. J. Wurman, P. Robinson, C. Alexander, Y. Richardson, Low-level winds in tornadoes and potential catastrophic tornado impacts in urban areas. *Bull. Am. Meteorol. Soc.* **88**, 31–46 (2007).
24. G. S. Forbes, R. M. Wakimoto, A concentrated outbreak of tornadoes, downbursts and microbursts, and implications regarding vortex classification. *Mon. Weather Rev.* **111**, 220–236 (1983).
25. R. J. Trapp, S. A. Tessendorf, E. S. Godfrey, H. E. Brooks, Tornadoes from squall lines and bow echoes. Part I: Climatological distribution. *Weather Forecast.* **20**, 23–34 (2005).
26. K. R. Knupp *et al*., Meteorological overview of the devastating 27 April 2011 tornado outbreak. *Bull. Am. Meteorol. Soc.* **95**, 1041–1062 (2014).
27. W. S. Ashley, A. M. Haberlie, J. Strohm, A climatology of quasi-linear convective systems and their hazards in the United States. *Weather Forecast.* **34**, 1605–1631 (2019).
28. R. M. Wakimoto, J. W. Wilson, Non-supercell tornadoes. *Mon. Weather Rev.* **117**, 1113–1140 (1989).
29. D. J. Novlan, W. M. Gray, Hurricane-spawned tornadoes. *Mon. Weather Rev.* **102**, 476–488 (1974).
30. L. A. Schultz, D. J. Cecil, Tropical cyclone tornadoes, 1950–2007. *Mon. Weather Rev.* **137**, 3471–3484 (2009).
31. J. M. Schoen, W. S. Ashley, A climatology of fatal convective wind events by storm type. *Weather Forecast.* **26**, 109–121 (2011).
32. A. K. Anderson-Frey, H. Brooks, Tornado fatalities: An environmental perspective. *Weather Forecast.* **34**, 1999–2015 (2019).
33. B. T. Smith, R. L. Thompson, J. S. Grams, C. Broyles, H. E. Brooks, Convective modes for significant severe thunderstorms in the contiguous United States. Part I: Storm classification and climatology. *Weather Forecast.* **27**, 1114–1135 (2012).
34. R. L. Thompson, B. T. Smith, J. S. Grams, A. R. Dean, C. Broyles, Convective modes for significant severe thunderstorms in the contiguous United States. Part II: Supercell and QLCS tornado environments. *Weather Forecast.* **27**, 1136–1154 (2012).
35. D. W. Burgess, M. A. Magsig, J. Wurman, D. C. Dowell, Y. Richardson, Radar observations of the 3 May 1999 Oklahoma City Tornado. *Weather Forecast.* **17**, 456–471 (2002).
36. J. C. Snyder, H. B. Bluestein, Some considerations for the use of high-resolution mobile radar data in tornado intensity determination. *Weather Forecast.* **29**, 799–827 (2014).
37. D. C. Dowell, C. Alexander, J. Wurman, L. Wicker, Centrifuging of scatterers in tornadoes. *Mon. Weather Rev.* **133**, 1501–1524 (2005).
38. American Society of Engineers (ASCE), Minimum design Loads for Buildings and other structures. *ASCE/SEI Standard 7-16* (ASCE 2020) (ASCE draft update of 2017 standard).
39. American Society of Engineers (ASCE), "Wind Speed Estimation in Tornadoes" in *Minimum Design Loads for Buildings and Other Structures. ASCE/SEI Standard 7-20* (ASCE draft).
40. W. C. Lee, J. Wurman, Diagnosed three-dimensional axisymmetric structure of the Mulhall tornado on 3 May 1999. *J. Atmos. Sci.* **62**, 2373–2393 (2005).
41. J. Wurman, S. Gill, Finescale radar observations of the dimmitt, Texas (2 June 1995), tornado. *Mon. Weather Rev.* **128**, 2135–2164 (2000).
42. R. M. Wakimoto, N. T. Atkins, J. Wurman, The Lagrange tornado during VORTEX2. Part I: Photogrammetric analysis of the tornado combined with single-Doppler radar data. *Mon. Weather Rev.* **139**, 2233–2258 (2011).
43. J. L. Houser, H. B. Bluestein, J. C. Snyder, A finescale radar examination of the tornadic debris signature and weak-echo reflectivity band Associated with a large, violent tornado. *Mon. Weather Rev.* **144**, 4101–4130 (2016).
44. R. M. Wakimoto, Z. Wienhoff, H. B. Bluestein, D. Reif, The dodge city tornadoes on 24 may 2016: Damage survey, photogrammetric analysis combined with mobile polarimetric radar data. *Mon. Weather Rev.* **146**, 3735–3771 (2018).
45. H. E. Brooks, On the relationship of tornado path length and width to intensity. *Weather Forecast.* **19**, 310–319 (2004).
46. R. P. Davies-Jones, The dependence of core radius on swirl ratio in a tornado simulator. *J. Atmos. Sci.* **30**, 1427–1430 (1973).
47. B. H. Fiedler, R. Rotunno, A theory for the maximum windspeeds in tornado-like vortices. *J. Atmos. Sci.* **43**, 2328–2340 (1986).
48. B. H. Fiedler, The thermodynamic speed limit and its violation in axisymmetric numerical simulations of tornado-like vortices. *Atmos.-Ocean* **32**, 335–359 (1994).
49. D. S. Nolan, A new scaling for tornado-like vortices. *J. Atmos. Sci.* **62**, 2639–2645 (2005).
50. D. S. Nolan, N. A. Dahl, G. H. Bryan, R. Rotunno, Tornado vortex structure, intensity, and surface wind gusts in large-eddy simulations with fully developed turbulence. *J. Atmos. Sci.* **74**, 1573–1597 (2017).
51. J. Wurman, The multiple-vortex structure of a tornado. *Weather Forecast.* **17**, 473–505 (2002).
52. H. B. Bluestein, W. Lee, M. Bell, C. C. Weiss, A. L. Pazmany, Mobile Doppler radar observations of a tornado in a supercell near bassett, Nebraska, on 5 June 1999. Part II: Tornado-vortex structure. *Mon. Weather Rev.* **131**, 2968–2984 (2003).
53. H. B. Bluestein *et al*., The structure of tornadoes near Attica, Kansas, on 12 may 2004: High-resolution, mobile, Doppler radar observations. *Mon. Weather Rev.* **135**, 475–506 (2007).
54. H. B. Bluestein, J. C. Snyder, J. B. Houser, A multiscale overview of the el reno, Oklahoma, tornadic supercell of 31 May 2013. *Weather Forecast.* **30**, 525–552 (2015).
55. C. B. Griffin, D. J. Bodine, J. M. Kurdzo, A. Mahre, R. D. Palmer, High-temporal resolution observations of the 27 May 2015 Canadian, Texas, tornado using the atmospheric imaging radar. *Mon. Weather Rev.* **147**, 873–891 (2019).
56. R. M. Wakimoto *et al*., Aerial Damage Survey of the, 2013 el reno tornado combined with mobile radar data. *Mon. Weather Rev.* **144**, 1749–1776 (2016).
57. J. M. Kurdzo, D. J. Bodine, B. L. Cheong, R. D. Palmer, High-temporal resolution polarimetric X-band Doppler radar observations of the 20 May 2013 moore, Oklahoma, tornado. *Mon. Weather Rev.* **143**, 2711–2735 (2015).
58. R. J. Trapp, G. R. Marion, S. W. Nesbitt, The regulation of tornado intensity by updraft width. *J. Atmos. Sci.* **74**, 4199–4211 (2017).

59. W. P. Winn, S. J. Hunyady, G. D. Aulich, Pressure at the ground in a large tornado. *J. Geophys. Res.* **104**, 22067–22082 (1999).
60. J. J. Lee, T. M. Samaras, C. R. Young, "Pressure Measurements at the Ground in an F-4 Tornado" in Presented at the AMS 22nd Conf. on Severe Local Storms (Amer. Meteor. Soc., Hyannis, MA, 2004), https://ams.confex.com/ams/pdfpapers/81700.pdf.
61. J. Wurman, T. Samaras, "Comparison of In-situ and DOW Doppler winds in a Tornado and RHI vertical slices through 4 Tornadoes during 1996–2004" in *Presented at the 22nd Conf. on Severe Local Storms* (Amer. Meteor. Soc., Hyannis, MA, 2004), https://ams.confex.com/ams/pdfpapers/82352.pdf.
62. S. Blair, D. Deroche, A. Pietrycha, In Situ Observations of the 21 April 2007 Tulia, Texas Tornado. *E-J. Severe Storms Meteorol.* **3**, https://ejssm.org/ojs/index.php/ejssm/article/viewArticle/39/42 (2008).
63. C. R. Alexander, J. Wurman, The 30 May 1998 Spencer, South Dakota, storm. Part I: The structural evolution and environment of the tornadoes. *Mon. Weather Rev.* **133**, 72–97 (2005).
64. J. Wurman, Y. Richardson, C. Alexander, S. Weygandt, P. F. Zhang, Dual-Doppler analysis of winds and vorticity budget terms near a tornado. *Mon. Weather Rev.* **135**, 2392–2405 (2007).
65. J. Wurman, Y. Richardson, C. Alexander, S. Weygandt, P. F. Zhang, Dual-Doppler and single-Doppler analysis of a tornadic storm undergoing mergers and repeated tornadogenesis. *Mon. Weather Rev.* **135**, 736–758 (2007).
66. J. Marquis, Y. Richardson, J. Wurman, P. Markowski, Single- and dual-Doppler analysis of a tornadic vortex and surrounding storm-scale flow in the Crowell, Texas, supercell of 30 April 2000. *Mon. Weather Rev.* **136**, 5107–5043 (2008).
67. K. Kosiba, R. J. Trapp, J. Wurman, An analysis of axisymmetric three-dimensional low-level wind field in a tornado using mobile radar observations. *Geophys. Res. Lett.* **35**, L5805 (2008).
68. J. Marquis, Y. Richardson, P. Markowski, D. Dowell, J. Wurman, Tornado maintenance investigated with high-resolution dual-Doppler and EnKF analysis. *Mon. Weather Rev.* **140**, 3–27 (2012).
69. J. Wurman *et al*., Finescale Single- and dual-Doppler analysis of tornado intensification, maintenance, and dissipation in the Orleans, Nebraska, supercell. *Mon. Weather Rev.* **138**, 4439–4455 (2010).
70. K. Kosiba, J. Wurman, The three-dimensional axisymmetric wind field structure of the Spencer, South Dakota, 1998 Tornado. *J. Atmos. Sci.* **67**, 3074–3083 (2010).
71. L. R. Lemon, C. A. Doswell, Severe thunderstorm evolution and mesocyclone structure as related to tornadogenesis. *Mon. Weather Rev.* **107**, 1184–1197 (1979).
72. D. W. Burgess, R. J. Donaldson Jr., P. R. Desrochers, "Tornado detection and warning by radar" in *The Tornado: Its Structure, Dynamics, Prediction and Hazards, Geophys. Monogr.* (Amer. Geophys Union, 1993), **Vol. 79**, pp. 203–221.